SCIENCE CHINA
Technological Sciences

• Article •

https://doi.org/10.1007/s11431-021-1873-9

# Design of an all-day electrical power generator based on thermoradiative devices

ZHANG Xin[1], YANG GuoFeng[1], YAN MengQi[1], ANG Lay Kee[2], ANG Yee Sin[2*] & CHEN JinCan[3*]

[1] *School of Science, Jiangnan University, Wuxi 214122, China;*
[2] *Science, Mathematics and Technology, Singapore University of Technology and Design, Singapore 487372, Singapore;*
[3] *Department of Physics, Xiamen University, Xiamen 361005, China*

Received April 1, 2021; accepted June 4, 2021; published online August 4, 2021

Energy harvesting from sun and outer space using thermoradiative devices (TRDs), despite being promising renewable energy sources, is limited only to daytime and nighttime period, respectively. Such a system with 24-hour continuous electric power generation remains an open question thus far. Here, a TRD-based power generator that harvests solar energy via concentrated solar irradiation during daytime and via thermal infrared emission towards the outer space at nighttime is proposed, thus achieving the much sought-after 24-hour electrical power generation. Correspondingly, a rigorous thermodynamical model is developed to investigate the all-day performance characteristics, parametric optimum design, and the role of various energy loss mechanisms. The calculated results predict that the daytime TRD-based system yields a peak efficiency of 12.6% under 10 suns, thus significantly outperforming the state-of-art record-setting solar thermoelectric generator. This work reveals the potential of TRD towards 24-hour electricity generation and future renewable energy technology.

**sustainable energy, HgCdTe, solar energy, thermoradiative, optimum design**

**Citation:** Zhang X, Yang G F, Yan M Q, et al. Design of an all-day electrical power generator based on thermoradiative devices. Sci China Tech Sci, 2021, 64, https://doi.org/10.1007/s11431-021-1873-9

## 1 Introduction

Developing renewable energy harvesting technologies capable of continuously operating throughout 24 h is strongly desirable, especially for supplying electricity to remote rural areas where access to electricity is challenging [1–7]. While solar power systems have offered a wide variety of electricity generation approaches, including photovoltaics [8–10] and solar thermal power systems [11, 12], the ability of generating electricity during both the daytime and nighttime with no necessity of energy storage remains an open question today. Serving as a omnipresent resource to almost all parts of Earth, the outer space is an easily accessible thermodynamic cold sink, whose role in renewable energy applications has been largely ignored until very recently. Energy harvesting utilizing the coldness of the outer space has been extensively explored as a new route towards renewable energy future [13, 14], for example, the concept of electric power generation using radiative sky cooling (RSC) and thermoelectric generators (TEGs) [15–17]. This concept of RSC has been experimentally demonstrated [16] via the coupling between the cold side of the TEG composed of a near-black surface that radiates thermal radiation to outer space and the hot side heated by ambient air. Similarly, all-day electricity generation using RSC and TEGs has also been actively explored [18–21]. While these recent experimental efforts concretely demonstrated the potential usefulness of energy harvesting from space, their performance is still limited by the relatively low figure of merit of thermoelectric materials.

*Corresponding authors (email: yeesin_ang@sutd.edu.sg; jcchen@xmu.edu.cn)

One feasible alternative to TEGs is to employ thermoradiative devices (TRDs) [22–25] that operate based on the thermoradiative effect of a semiconductor photodiode. The TRD is an emerging heat-to-electricity technique that radiates a fraction of above-bandgap thermal radiation to the cold environment when operates at higher temperatures, and consequently, electrical power generation is achieved via photon exchange [24]. Different from RSC, the TRD, a semiconductor photodiode, undergoing radiative exchange with a colder object, can generate electric power by harvesting the outgoing thermal radiation from the diode. This negative illumination effect is in contrast with a usual "positive illumination" mode of operation for energy harvesting, such as the operation of a solar cell, where the photodiode harvests incoming thermal radiation from a hotter object. Experimentally, a thermoradiative semiconductor photodiode based on HgCdZnTe generates up to 1 pW of electrical power, which is insufficient for practical applications [26]. To further improve the ability of power generation beyond the pW scale, we take the advantages of the naturally-existed temperature difference between the Sun, the environment, and the outer space to generate larger temperature difference. Thus, increasing the output electrical power could be a feasible approach [27–29]. However, a number of open questions remain unaddressed so far: (i) Can the concentrated solar thermal power and the thermoradiative effect be synnergized for harvesting energy from both sun and the outer space? (ii) How to construct a rigorous computational model to understand the performance of such system in the presence of realistic optical, electric, and thermal losses? (iii) Which loss mechanism is the most dominant in limiting the system performance? (iv) What is the thermodynamic bounds of the system performance, and the optimal design strategies that can be applied to mitigate the effects that negatively impact the system performance?

In this paper, the above questions are addressed by computationally designing a energy conversion system that couples a nighttime thermoradiative system with a daytime concentrated solar thermal power to produce electricity continuously throughout 24 h. Such system is capable of providing small-scale, distributed renewable power generation for 24 h a day and its performance is uniquely enabled by the optical coupling among Sun, outer space, and Earth's ambient environment.

## 2 Model and methods

Figure 1(a) shows an improved design of all-day thermoradiative system configuration that employs a three-dimensional structured graphene metamaterial (3D-SGM) solar absorber, a TRD based on a HgCdTe p-n junction, and an Ag back surface reflector (BSR) under a parallel-plate geometry. The Sun (~6000 K), the environment near the Earth's surface (~300 K), and the outer space (~3 K) are three separate locations with a large temperature difference. Radiative heat transfer links the three thermodynamic resources through solar heating and thermal infrared radiation. During the daytime, the easily accessible sunlight serves as a heat source, and the ambient air acts as a cold sink to establish a consider temperature difference (~5700 K). An optical reflector allows the concentrated sunlight to impinge on the solar absorber, which convert entire solar spectrum into heat. The TRD absorbs a portion of the input thermal energy and operates at the temperature range of 500–800 K, generating electricity via photon exchange with the cold environment. At night, employing the warm environment as the heat reservoir and the outer space as the cold sink, the TRD radiates photons into the cold space through the atmospheric transparency window to generate electric power. A spectrum-selective mirror located on the right side reflects the infrared thermal emission, meanwhile, is transparent for other wavelength range so that the non-infrared radiation from the TRD can be emitted into the environment. Thus, the system does not incur additional daily power consumption to reconfigure the system mechanically. The solar absorber is modeled based on a representative design of 3D-SGM with period 0.8 μm, trench depth 1 μm, hole width 0.59 μm, and film thickness 30 nm as reported in ref. [30].

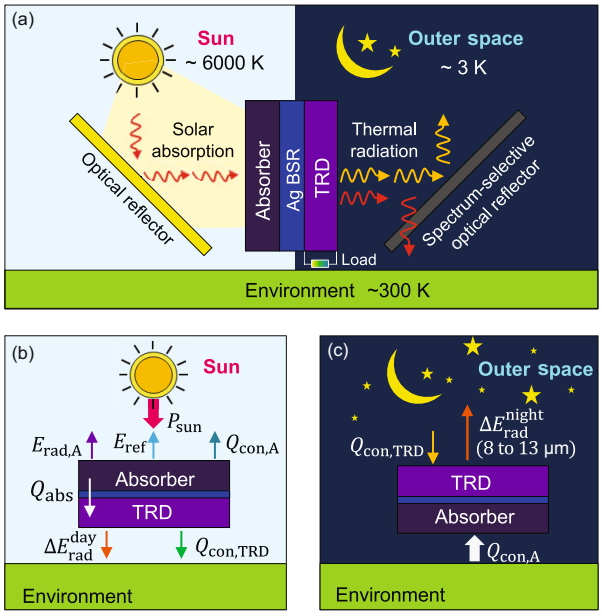


**Figure 1** (Color online) (a) Schematic of a 24-hour TRD system for continuous electricity generation by optically coupling with the Sun, outer space, and environment; (b) and (c) correspond the energy flow diagram of daytime and nighttime TRD system.

### 2.1 Daytime concentrated TRD systems

For simplicity, the subscripts "A" and "E" are used to denote absorber and environment, respectively. At daytime, the solar-to-electric conversion efficiency of the system is defined as

$$\eta = \frac{P}{P_{\text{sun}}} = \frac{JV}{C\int_0^\infty \mathcal{I}_{\text{AM1.5D}}(\lambda)\,\mathrm{d}\lambda}, \tag{1}$$

where $P = JV$ represents the output electric power density, $J$ is the current density, and $V$ is the output voltage. $P_{\text{sun}}$ is the concentrated solar power flux impinging on the top surface of the absorber. $\mathcal{I}_{\text{AM1.5D}}$ represents the AM1.5D solar irradiance varying with the wavelength $\lambda$ (Figure 2(a)). $C$ denotes the solar concentration factor. The overall efficiency is also the product of the optothermal efficiency of the absorber ($\eta_{\text{ot}}$) and the thermoelectric conversion efficiency of the TRD ($\eta_{\text{TRD}}$), i.e., $\eta = \eta_{\text{ot}} \cdot \eta_{\text{TRD}}$. Here $\eta_{\text{ot}} = Q_{\text{abs}}/P_{\text{sun}}$ characterizes the solar-to-thermal conversion capacity of the absorber that converts the concentrated solar power flux into heat flux that flows into the TRD ($Q_{\text{abs}}$) and $\eta_{\text{TRD}}$ is defined as the ratio of the output electric power density to the incoming heat flux, i.e., $\eta_{\text{TRD}} = P/Q_{\text{abs}}$.

In the TRD, considering the effect of non-radiative (NR) process, the current density is given by [22, 24, 25]

$$J = e[N_{\text{abs}}(0, T_{\text{E}}) - N_{\text{em}}(\Delta\mu, T_{\text{TRD}})] - J_{\text{NR}}(\Delta\mu, T_{\text{TRD}}), \tag{2}$$

where $N(\Delta\mu, T) = \frac{c}{4\pi}\int_0^{\lambda_{\text{g}}} \epsilon_{\text{TRD}}(\lambda) D(\lambda) \Theta(\Delta\mu, T)\,\mathrm{d}\lambda$ is the photon flux, $e$ is the electron charge, $c$ is the speed of light in vacuum, $T$ is the temperature, $\lambda_{\text{g}}$ is the cut-off wavelength corresponding to the semiconductor bandgap $E_{\text{g}}$, $\epsilon_{\text{TRD}}(\lambda)$ is the emissivity of the TRD or HgCdTe surface and, according to Kirchhoff's law, is equal to the absorptivity, and $D(\lambda) = 1/(c\pi^2\lambda^2)$ is the photon density of states in a homogeneous bulk material. $\Theta(\Delta\mu, T) = 1/[\mathrm{e}^{(\hbar c\lambda - \Delta\mu)/k_{\text{B}}T} - 1]$ is the modified Bose-Einstein distributions of photons, and $\Delta\mu = eV$ is the chemical potential driving photon emission. The first term in eq. (2) is related to the above-bandgap photon flux. The corresponding net radiative energy flux from the TRD to the environment is $\Delta E_{\text{rad}}^{\text{day}} = E_{\text{em}}^{\text{day}}(\Delta\mu, T_{\text{TRD}}) - E_{\text{abs}}^{\text{day}}(0, T_{\text{E}})$, where $E^{\text{day}}(\Delta\mu, T) = \frac{\hbar c^2}{4\pi}\int_0^{\lambda_{\text{g}}} \frac{\epsilon_{\text{TRD}}(\lambda) D(\lambda) \Theta(\Delta\mu, T)}{\lambda}\,\mathrm{d}\lambda$. To quantitatively describe the non-radiative loss, including the Auger and Shockley-Read-Hall (SRH) process, the net current losses generated in the high-injection regime can be calculated as [31]

$$J_{\text{NR}}(\Delta\mu, T) = et\left[\tau_{\text{auger}} n_i^3 \exp\left(\frac{3\Delta\mu}{2k_{\text{B}}T}\right) + \frac{n_i^2}{\tau_{\text{SRH}}} \exp\left(\frac{\Delta\mu}{2k_{\text{B}}T}\right)\right], \tag{3}$$

where $t$ denotes the thickness of the active region, $\tau_{\text{auger}}$ represents the intrinsic Auger recombination times, $n_i$ is intrinsic carrier concentration, and $\tau_{\text{SRH}} = 1$ μs is the bulk Shockley-Read-Hall lifetime based on the experimental measurements [32]. The temperature dependence of $\tau_{\text{auger}}$ and $n_i$ is determined by [33, 34]

$$\tau_{\text{auger}}(T) = 8.3 \times 10^{-13} E_{\text{g}}^{0.5} (e/k_{\text{B}}T)^{1.5} e^{E_{\text{g}}/k_{\text{B}}T} \tag{4}$$

and

$$n_i(x, T) = (5.585 - 3.82x + 0.001753T - 0.001364xT) \times 10^{14} E_{\text{g}}^{0.75} T^{1.5} \mathrm{e}^{-E_{\text{g}}/2k_{\text{B}}T}. \tag{5}$$

Eq. (3) illustrates that the non-radiative recombination is a volumetric effect because the number of non-radiative recombination events per unit area is proportional to the device's thickness. A thickness of $t = 100$ nm [34] is chosen, such that there is sufficient thickness for photon absorption while the layer remains thin enough to mitigate the non-radiative effect. The temperature-dependent bandgap of $\mathrm{Hg}_{1-x}\mathrm{Cd}_x\mathrm{Te}$ compounds is also considered, which can be described as

$$E_{\text{g}}(x, T) = -0.312 + 1.93x - 0.81x^2 + 0.832x^3 + 5.35 \times 10^{-4}(1 - 2x)T. \tag{6}$$

The conversion efficiency and current density can be calculated from eqs. (1)–(5) once the TRD's temperature is determined from the energy balance condition. Taking into account all the power fluxes involving the absorber and TRD (Figure 1(b)), one can obtain

$$P_{\text{sun}} - E_{\text{rad,A}} - E_{\text{ref}} - Q_{\text{con,A}} - Q_{\text{abs}} = 0, \tag{7a}$$

$$Q_{\text{abs}} - \Delta E_{\text{rad}}^{\text{day}} - Q_{\text{con,TRD}} - P = 0, \tag{7b}$$

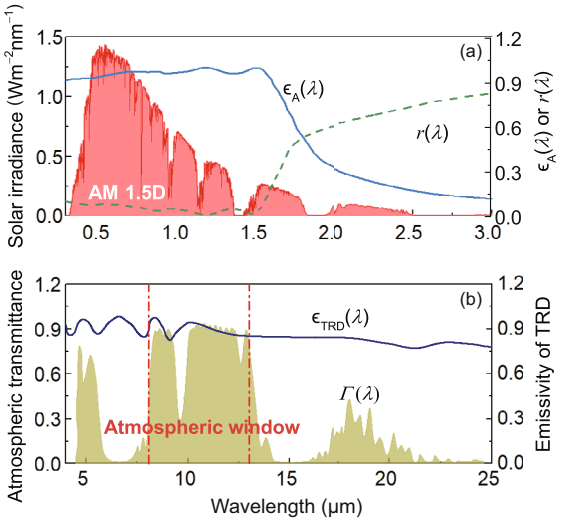


**Figure 2** (Color online) Optical properties of the components in the system. (a) The solar irradiance of AM1.5D solar spectrum, spectral emissivity $\epsilon_{\text{A}}(\lambda)$ and reflectance $r_{\text{A}}(\lambda)$ of the 3D SGM absorber; (b) atmospheric transmittance $\Gamma(\lambda)$ and emissivity of the TRD $\epsilon_{\text{TRD}}(\lambda)$ varying with the wavelength, where wavelength range from 8 to 13 μm corresponds to atmospheric window.

where $E_{\mathrm{rad,A}} = \frac{2\pi\hbar c^2}{\int_0^\infty \epsilon_{\mathrm{A}}(\lambda)[\Theta(T_{\mathrm{A}})-\Theta(T_{\mathrm{E}})]\lambda^5\,\mathrm{d}\lambda}$ is the blackbody thermal radiation flux from the absorber into the environment, $\epsilon_{\mathrm{A}}(\lambda)$ is the emissivity of the absorber's top surface, $E_{\mathrm{ref}} = C\int_0^\infty r(\lambda)\mathit{I}_{\mathrm{AM1.5D}}(\lambda)\,\mathrm{d}\lambda$ is the reflected radiation flux of the absorber, $r(\lambda) = 1-\epsilon_{\mathrm{A}}(\lambda)$ represents the spectral reflectance (see Figure 2(a)), $Q_{\mathrm{con,A}} = h_{\mathrm{A}}(T_{\mathrm{A}} - T_{\mathrm{E}})$ ($Q_{\mathrm{con,TRD}} = h_{\mathrm{TRD}}(T_{\mathrm{TRD}} - T_{\mathrm{E}})$) is the heat flux caused by heat convection and conduction between the absorber (TRD) and the environment according to the Newton heat transfer law, and $h_{\mathrm{TRD}} = h_{\mathrm{A}} = 7\ \mathrm{W\ m^{-2}\ K^{-1}}$ is the corresponding global heat transfer coefficient that is compatible to the standard air conditions. It should be noted that the radiative energy flux from the TRD into the outer space via the atmospheric transparency window could affect the daytime operation of the TRD system. Like the working principle of RSC to dissipate heat, such a portion of radiative flux at the wavelength range of 8–13 μm can also cool down the TRD's temperature via radiative cooling and degrade device performance. However, compared with the above-bandgap photon radiative flux, the radiative flux with the wavelength range of 8–13 μm is relatively low. It can be assumed that the effect of TRD's ability to dissipate heat in the 8–13 μm window into outer space on its daytime operation is not considered in this work.

### 2.2 Nighttime TRD systems

At nighttime, the TRD system enables electric power generation by coupling the cold outer space with the warm ambient environment through the atmospheric transparency window. The current density is given by [35]

$$J = e[\epsilon_{\mathrm{atm}}(\lambda)F_{\mathrm{abs}}(0,T_{\mathrm{atm}}) + (1-\epsilon_{\mathrm{atm}}(\lambda))F_{\mathrm{abs}}(0,T_{\mathrm{space}}) - F_{\mathrm{em}}(\Delta\mu,T_{\mathrm{TRD}})] - J_{\mathrm{NR}}(\Delta\mu,T_{\mathrm{TRD}}), \tag{8}$$

where

$$F(\Delta\mu,T) = \frac{c}{4\pi}\int_{8\mu\mathrm{m}}^{13\mu\mathrm{m}} \epsilon_{\mathrm{TRD}}(\lambda)D(\lambda)\Theta(\Delta\mu,T)\,\mathrm{d}\lambda \tag{9}$$

is the photon flux at wavelength range of 8–13 μm. The angle-dependent emissivity of the atmosphere is given by $\epsilon_{\mathrm{atm}}(\theta,\lambda) = 1-\Gamma(\lambda)^{1/\cos\theta}$, where $\Gamma(\lambda)$ is the atmospheric transmittance in the zenith direction as obtained from MODTRAN5 [36], $\theta$ is the average solid angle of 35° [35]. $T_{\mathrm{atm}}$ and $T_{\mathrm{space}}$ are the temperatures of the atmosphere (298 K) and outer space (3 K), respectively. In eq. (8), the 1st, 2nd, and 3rd terms in the braces are the incoming photon flux from the atmosphere, the incoming photon flux from the outer space, which is mostly in atmospheric transparency window (8–13 μm), and the outgoing photon flux from the TRD, respectively.

The power conversion efficiency can be expressed as

$$\eta = \frac{JV}{JV + \Delta E_{\mathrm{rad}}^{\mathrm{night}} + Q_{\mathrm{con,TRD}}}, \tag{10}$$

where

$$\Delta E_{\mathrm{rad}}^{\mathrm{night}} = E_{\mathrm{em}}^{\mathrm{night}}(\Delta\mu,T_{\mathrm{TRD}}) - E_{\mathrm{abs}}^{\mathrm{night}}(0,T_{\mathrm{atm}}) - E_{\mathrm{abs}}^{\mathrm{night}}(0,T_{\mathrm{space}}) \tag{11}$$

is the net radiative energy flux among the TRD, outer space, and atmosphere. In eq. (11), the nighttime radiative energy flux $E^{\mathrm{night}}$ is given by

$$E^{\mathrm{night}} = \frac{\hbar c^2}{4\pi}\int_{8\ \mu\mathrm{m}}^{13\ \mu\mathrm{m}} \frac{\epsilon_{\mathrm{TRD}}(\lambda)D(\lambda)\Theta(\Delta\mu,T)}{\lambda}\,\mathrm{d}\lambda. \tag{12}$$

In the nighttime temperature range, the incoming photon flux from the outer space can be neglected, because the spectral irradiance from 3 K black body is extremely low.

The operating temperature of the TRD is assumed to be the same as that of the solar absorber, i.e., $T_{\mathrm{TRD}} = T_{\mathrm{A}}$, because the high-melting materials with ultrahigh thermal conductivity are usually filled between them. A mole fraction of $x = 0.12$ for $Hg_{1-x}Cd_xTe$ is selected, which corresponds to a low bandgap of 0.05 to 0.08 eV at the temperature range of 300–800 K, which enables significant above-bandgap emissivity in the atmospheric transparency window (0.09–0.15 eV) [34].

## 3 Results and discussion

The all-day TRD system is modeled and its theoretical performance limit is determined based on the following assumptions: (i) The optical properties such as the emissivity and reflectivity are independent of temperature. While real materials' optical properties are all temperature dependent, the assumption of temperature independent properties will allow identification of key parameters affecting the system performance. Analysis based on temperature dependent properties will be presented in the future. (ii) The device's materials keep stable under cyclic temperature variation. (iii) Adhesion, electrical and thermal contact resistances are negligible. The effects of those factors inevitably exist in the actual device. This approximation is made to allow us focusing on predicting the best performance of the all-day TRD-based system. These assumptions are consistent with all of the previously established theoretical limit for solar energy harvesting [37–39] and outgoing thermal radiation harvesting [10,22,24–29].

Figure 2 shows the optical properties of the components in the all-day TRD system, such as normalized AM1.5D solar spectrum, 3D SGM, the mid-infrared atmospheric transparency window, and HgCdTe. The nearly unity absorptivity

(~0.96) in the solar irradiance region (0.3 to 1.6 μm) ensures an excellent absorption of sunlight to heat up the TRD module under the Sun. The low reflectance allows the efficient absorbtion of most of the concentrated sunlight. Importantly, 3D-SGM absorber exhibits these unique features, such as the superior selective absorption for solar spectrum, flexible tunability of wavelength-selective absorption, high thermal stability, and excellent opto-thermal performance, which are particularly beneficial for designing high-performance solar-thermal energy harvesting device. Additionally, an excellent emissivity $\epsilon_{\mathrm{TRD}}$ of HgCdTe (around 0.9) in the atmospheric transparency window ensures thermal infrared radiation with outer space.

Using eqs. (1)–(7), the performance characteristics of the daytime TRD system are simulated realistically (Figure 3(a) and (b)). Figure 3(a) shows the efficiency of the daytime TRD system and subsystems as a function of the output voltage. Individually, the opto-thermal efficiency and the TRD's efficiency reach 92.8% and 18.5%, respectively, thus revealing the TRD as the bottleneck that limits the conversion efficiency during daytime operation. The product of these two individual efficiencies, i.e., 78.2% and 16.1%, yields the combined peak efficiency of 12.6% under 10 suns. Figure 3(b) obtains the volt-ampere characteristic curve of the daytime TRD system. The current density decreases with an increasing output voltage, and the system exhibits an open-circuit voltage of −0.168 V and a short-circuit current density of −6.32 A cm$^{-2}$. Here the operating current density and voltages have opposite signs in contrast to photovoltaic cell because the radiative processes are reciprocal. Since the energy exchange of the TRD is closely dependent on the net radiative energy fluxes from the TRD, the TRD's temperature decreases at higher output voltages (Figure 3(b)) to satisfy the energy balance in eq. (4), where the radiative energy fluxes transported from the TRD to the environment are substantially lower.

Furthermore, the process that contributes to the major energy losses in the TRD is identified. The peak efficiencies of the system are calculated in four cases, including (1) the ideal system, (2) the system with only the optical loss, (3) the system with only the non-radiative loss, (4) the system with only the heat conduction and convection loss. The corresponding values are 28.6%, 25.4%, 22.9%, 27.3%. Compared with the proposed system with all losses (12.6%), the non-radiative recombination is a main loss mechanism that significantly degrades the daytime TRD system performance. The ongoing research efforts suppress the Auger process using quantum wells, doping profile control, superlattices, or heterostructures and, meanwhile, mitigate surface recombination by passivation. Moreover, to reduce the optical loss, a back-reflector metallic grating (Ag mirror) can be used to promote light utilization in the active layer, which is thermally conducting on the bottom surface. A device module encapsulation can also be used to protect the system from the environment and to restrict conductive and convective heat loss.

Next, how different solar concentration factors can affect the optimal performance characteristics of the daytime TRD system is investigated, as shown in Figure 4(a), where the voltage has been optimized. In general, larger solar concentrations correspond to more input energy fluxes, and thus lead to higher peak efficiencies ($\eta_{\max}$) and corresponding TRD's temperatures ($T_{\mathrm{TRD}}^{\mathrm{opt}}$). From a theoretical point of view, if does not consider material limits, the peak efficiency first increases and then decreases with the solar concentration factor. Actually, at exceptionally high solar concentration, the semiconductor component of the system can be severely damaged by high temperature which could lead to saturate or even downgrade of peak efficiency at overly high solar concentration factor. Because of this, the solar concentration factor is limited to the range of 5 to 15, which corresponds to a temperature range of about 500 to 800 K. Such temperature range is still manageable for used semiconductor materials, such as HgCdTe, which has a melting point as high as 1000 K. In addition, the optimal current density ($J_{\mathrm{opt}}$) and output voltage ($V_{\mathrm{opt}}$) decrease with solar concentrations (Figure 4(b)). Further increment in overall efficiency is possible with higher

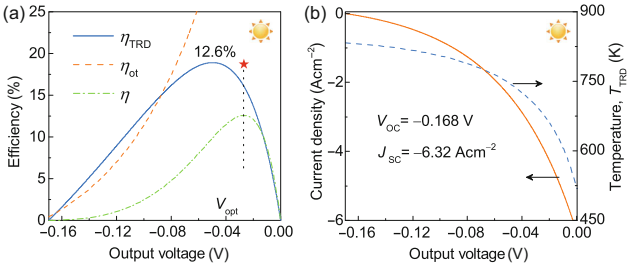


**Figure 3** (Color online) (a) The opto-thermal efficiency $\eta_{\mathrm{ot}}$, TRD's efficiency $\eta_{\mathrm{TRD}}$, and overall efficiency $\eta$; (b) current density $J$ and TRD's temperature $T_{\mathrm{TRD}}$ as functions of the negative output voltage $V$ in the daytime TRD system under 10 suns.

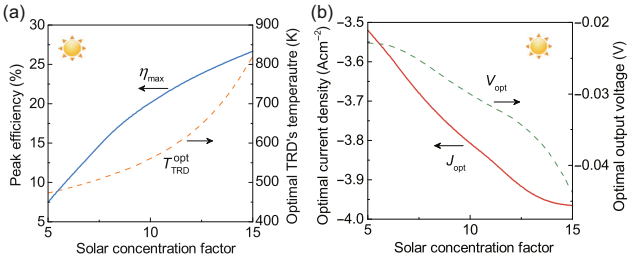


**Figure 4** (Color online) (a) The peak efficiency ($\eta_{\max}$) and corresponding TRD's temperature ($T_{\mathrm{TRD}}^{\mathrm{opt}}$); (b) optimal current density ($J_{\mathrm{opt}}$) and output voltage ($V_{\mathrm{opt}}$) under different solar concentration factors.

optical concentration for the daytime TRD system to operate at higher temperatures.

The peak efficiencies and the corresponding working temperatures are also compared between the daytime TRD system and the concentrated TEG-based solar cell, in which a peak efficiency of 6% and 520 K has been theoretically achieved [37]. The theoretically predicted values of the daytime TRD system, i.e., 8% and 520 K when irreversible losses are included, are higher than TEG-based solar cells. These performance figure of merits demonstrate the potential advantageous of daytime TRD system in solar-to-electric energy conversion. The TEG is a solid state device that converts heat flux (temperature differences) directly into electrical energy through the Seebeck effect. Its conversion efficiency (around 5%–8%) is significantly limited by low figure of merit of thermoelectric materials. Besides low efficiency and relatively high cost, practical problems exist in applications resulting from a relatively high electrical output resistance, which increases self-heating, and a relatively low thermal conductivity, which makes them unsuitable for applications where heat removal is critical, as with heat removal from an electrical device. Compared with the TEG, the TRD possesses the advantageous characteristics on account of the large power density, relatively simple design and operation, and low-cost manufacturing. The TRD converts part of the supplied heat from the heat source into electricity via photon exchanges with surroundings under negative illumination. The method is based on sustaining a difference in the chemical potential for electron populations above and below an energy gap and let this difference drive a current through an electric circuit. The difference in chemical potential originates from an imbalance in the excitation and de-excitation of electrons across the energy gap.

The operation of the TRD system at nighttime is different from that at daytime. In the latter, the state of the maximum efficiency coincides with that of the maximum power density (MPD) because the efficiency is defined as the ratio of the output electric power to the total incident power per unit area, which is a given quantity (~1003 W $m^{-2}$). For nighttime TRD operation, the absorbed heat flux is variable and is closely dependent on the parameters of the TRD, such as the voltage and bandgap. The power density exhibits a non-monotonous dependence with the output voltage (Figure 5(a)). In contrast, the conversion efficiency decreases monotonously with the output voltage because the input heat flux or TRD's temperature increases with the output voltage. The numerical results reveal that the nighttime TRD system operating at 293 K, can generate a MPD of 0.81 W $m^{-2}$ for a voltage of −0.026 V, while yielding a corresponding efficiency of 7.5%. The detailed-balance analysis here thus points to significant room for improvement in the negative illumination concept. This MPD is still lower than that of the Shockley-Queisser limit in negative illumination (54.8 W $m^{-2}$ (ref. [27]) and 3.99 W $m^{-2}$ (ref. [35])), where the effect of the atmosphere is considered and not considered, respectively. The relatively small value comes from more comprehensive consideration of non-radiative recombination and temperature-dependent parameters for semiconductor materials. If we can reduce the responsivity in the wavelength range outside the transparency window while keeping the external quantum efficiency (EQE) of 1, the achievable output power density would approach the Shockley-Queisser limit of negative illumination. Fortunately, the predicted MPD in our work agrees reasonably well with the previous value of ref. [35], i.e., 8.85 W $m^{-2}$ with EQE of 0.14. This indicates that if the EQE is increased, the power density can be significantly improved. Figure 5(b) shows the volt-ampere characteristic curve of the nighttime TRD system. The current density increases with the increment of the output voltage, and the system exhibits an open-circuit voltage of −0.11 V and a short-circuit current density of −88.6 A $m^{-2}$.

It is further noted that the MPD and the corresponding optimal values of the TRD temperature, current density, and output voltage are depended on the temperature of the ambient environment. Taking MPD as the key objective function, it is found that the MPD and the TRD temperature monotonically increases with increasing temperature in the range of 280 to 350 K (Figure 6(a)). In addition, the optimal current density and output voltage decrease with environment temperature (Figure 6(b)). Comparing the nighttime TRD system with the nighttime TEG radiative cooling system based on a commercial TEG module (TG12-4-01LS, Marlow Industries) [16], the MPD of the nighttime TRD system proposed here is 0.81 W $m^{-2}$ at 293 K, which is substantially higher than 52 mW $m^{-2}$ [15] and 20 mW $m^{-2}$ [17] at room temperature of the nighttime TEG system. It is noted that the proposed implementation has another good advantage over the previously nighttime

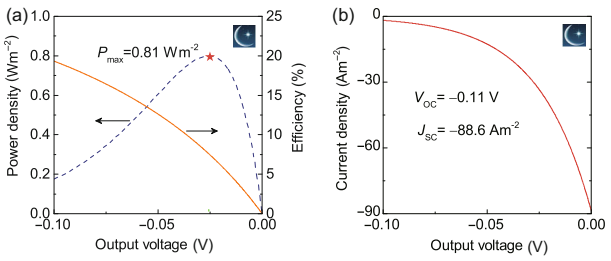


**Figure 5** (Color online) Nighttime at 293 K. (a) The power density $P$ and conversion efficiency $\eta$; (b) current density $J$ and TRD's temperature $T_{TRD}$ as functions of the negative output voltage $V$.

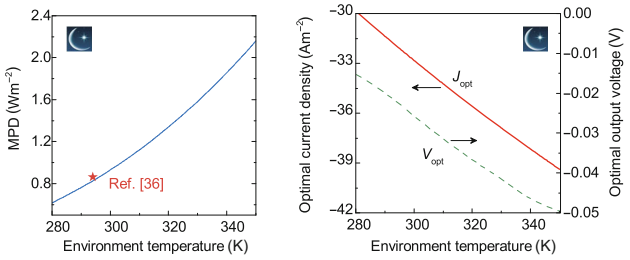


**Figure 6** (Color online) Nighttime. (a) The MPD and corresponding TRD's temperature ($T_{TRD}^{opt}$); (b) optimal current density ($J_{opt}$) and output voltage ($V_{opt}$) under different environment temperatures.

TEG radiative cooling system, because the TRD integrates both the electric power generation and RSC functions into one component. Such a simplified system structure can avoid the contact thermal resistance that would exist in the TEG radiative cooling implementation. The above comparisons suggest the superior nighttime energy harvesting performance of the proposed TRD system.

The current study focuses on developing a thermodynamical model of all-day TRD system to investigate its steady-state performance characteristics, parametric optimum design, and the role of various energy loss mechanisms under fixed irradiation and ambient conditions. But realistically, the solar irradiation, ambient temperature, and relative humidity vary throughout the 24-hour a day, a computational model that takes into account all realistic effects, as suggested by the reviewer, is beyond the scope of this work. A more comprehensive theoretical model of the all-day thermoradiative system to analyze the 24-hour performance calls for extra investigations in the future studies.

## 4 Conclusion

In summary, a high-performance 24-hour TRD system is proposed that enabled by HgCdTe p-n junctions for 24-hour harvesting energy from the sun and outer space. The daytime system yields a peak efficiency of 12.6% under low concentration factors, which significantly outperformed other representative TEG-based solar energy harvesting devices. The nighttime system has a MPD of 0.81 W m$^{-2}$ at 293 K, which is also higher than that of the nighttime TEG-based system. The device model developed above and the device performance characteristics outlined in Figures 3–6 shall offer an important design guideline for developing high-performance TRD-based energy converters. The results demonstrate TRD as a viable alternative route towards off-grid and battery-free renewable energy source.

*This work was supported by the Fundamental Research Funds for the Central Universities of China (Grant No. JUSRP121049) and the National Natural Science Foundation of China (Grant No. 12075197). The Authors acknowledge the insightful suggestions from the anonymous reviewer(s).*

1 Cabraal R A, Barnes D F, Agarwal S G. Productive uses of energy for rural development. Annu Rev Environ Resour, 2005, 30: 117–144
2 Chen L G, Meng F K, Ge Y L, et al. Performance optimization of a class of combined thermoelectric heating devices. Sci China Tech Sci, 2020, 63: 2640–2648
3 Ding Z M, Chen L G, Ge Y L, et al. Optimal performance regions of an irreversible energy selective electron heat engine with double resonances. Sci China Tech Sci, 2019, 62: 397–405
4 Lin B H, Huang Z F. Optimization of irreversible capacitive thermoelectric conversion device performance (in Chinese). Sci Sin Tech, 2020, 50: 551–561
5 Qiu S S, Ding Z M, Chen L G, et al. Performance optimization of thermionic refrigerators based on van der Waals heterostructures. Sci China Tech Sci, 2021, 64: 1007–1016
6 Song Y H, Chen X S, Lin J, et al. Stochastic processes in renewable power systems: From frequency domain to time domain. Sci China Tech Sci, 2019, 62: 2093–2103
7 Zhang Y W, Lu Y N, Chen L Q. Energy harvesting via nonlinear energy sink for whole-spacecraft. Sci China Tech Sci, 2019, 62: 1483–1491
8 Fang R, Zhang W J, Zhang S S, et al. The rising star in photovoltaics-perovskite solar cells: The past, present and future. Sci China Tech Sci, 2016, 59: 989–1006
9 Lin B H, Liao T J. Investigation on the performance of a photon-enhanced thermionic emission solar cell (in Chinese). Sci Sin Tech, 2019, 49: 873–879
10 Zhang X, Wang J C, Ang L K, et al. Designing few-layer graphene Schottky contact solar cells: Theoretical efficiency limits and parametric optimization. Appl Phys Lett, 2021, 118: 053103
11 Cheng X T, Xu X H, Liang X G. Theoretical analyses of the performance of a concentrating photovoltaic/thermal solar system with a mathematical and physical model, entropy generation minimization and entransy theory. Sci China Tech Sci, 2018, 61: 843–852
12 Han X, Xu C, Pan X Y, et al. Dynamic analysis of a concentrating photovoltaic/concentrating solar power (CPV/CSP) hybrid system. Sci China Tech Sci, 2019, 62: 1987–1998
13 Cheng Z M, Shuai Y, Gong D Y, et al. Optical properties and cooling performance analyses of single-layer radiative cooling coating with mixture of $TiO_2$ particles and $SiO_2$ particles. Sci China Tech Sci, 2021, 64: 1017–1029
14 Yin X B, Yang R G, Tan G, et al. Terrestrial radiative cooling: Using the cold universe as a renewable and sustainable energy source. Science, 2020, 370: 786–791
15 Fan L, Li W, Jin W, et al. Maximal nighttime electrical power generation via optimal radiative cooling. Opt Express, 2020, 28: 25460–25470
16 Raman A P, Li W, Fan S. Generating light from darkness. Joule, 2019, 3: 2679–2686
17 Zhao B, Pei G, Raman A P. Modeling and optimization of radiative cooling based thermoelectric generators. Appl Phys Lett, 2020, 117: 163903
18 Chen Z, Zhu L X, Li W, et al. Simultaneously and synergistically harvest energy from the sun and outer space. Joule, 2019, 3: 101–110
19 Ishii S, Dao T D, Nagao T. Radiative cooling for continuous thermoelectric power generation in day and night. Appl Phys Lett, 2020, 117: 013901
20 Tian Y P, Liu X J, Chen F Q, et al. Harvesting energy from sun, outer space, and soil. Sci Rep, 2020, 10: 20903
21 Xia Z L, Zhang Z F, Meng Z H, et al. A 24-hour thermoelectric generator simultaneous using solar heat energy and space cold energy. J Quantitative Spectr Radiative Transfer, 2020, 251: 107038
22 Fernández J J. Theoretical optimization of the working properties of

spatial thermoradiative cells using the Carnot efficiency. J Appl Phys, 2019, 125: 103101
23 Lin B H, Liao T J. Thermoradiative-thermionic hybrid energy electron devices. IEEE Trans Electron Devices, 2020, 67: 1132–1135
24 Strandberg R. Theoretical efficiency limits for thermoradiative energy conversion. J Appl Phys, 2015, 117: 055105
25 Zhang X, Ang Y S, Chen J, et al. Design of an InSb thermoradiative system for harvesting low-grade waste heat. Opt Lett, 2019, 44: 3354–3357
26 Santhanam P, Fan S. Thermal-to-electrical energy conversion by diodes under negative illumination. Phys Rev B, 2016, 93: 161410
27 Buddhiraju S, Santhanam P, Fan S. Thermodynamic limits of energy harvesting from outgoing thermal radiation. Proc Natl Acad Sci USA, 2018, 115: 3609–3615
28 Deppe T, Munday J N. Nighttime photovoltaic cells: Electrical power generation by optically coupling with deep space. ACS Photonics, 2019, 7: 1–9
29 Li W, Buddhiraju S, Fan S. Thermodynamic limits for simultaneous energy harvesting from the hot sun and cold outer space. Light Sci Appl, 2020, 9: 68
30 Lin K T, Lin H, Yang T S, et al. Structured graphene metamaterial selective absorbers for high efficiency and omnidirectional solar thermal energy conversion. Nat Commun, 2020, 11: 1–10
31 Burger T, Fan D, Lee K, et al. Thin-film architectures with high spectral selectivity for thermophotovoltaic cells. ACS Photonics, 2018, 5: 2748–2754
32 Rogalski A. HgCdTe infrared detector material: History, status and outlook. Rep Prog Phys, 2005, 68: 2267–2336
33 Hansen G L, Schmit J L. Calculation of intrinsic carrier concentration in $Hg_{1-x}Cd_xTe$. J Appl Phys, 1983, 54: 1639–1640
34 Zhang X, Du J Y, Chen J C, et al. Designing high-performance nighttime thermoradiative systems for harvesting energy from outer space. Opt Lett, 2020, 45: 5929–5932
35 Ono M, Santhanam P, Li W, et al. Experimental demonstration of energy harvesting from the sky using the negative illumination effect of a semiconductor photodiode. Appl Phys Lett, 2019, 114: 161102
36 Berk A, Anderson G P, Acharya P K, et al. Modtran5: 2006 update. In: Proceedings of SPIE, 2006. 62331F
37 Chen G. Theoretical efficiency of solar thermoelectric energy generators. J Appl Phys, 2011, 109: 104908
38 Harder N P, Wuerfel P. Theoretical limits of thermophotovoltaic solar energy conversion. Semicond Sci Technol, 2003, 18: S151–S157
39 Liao T J, Zhang X, Chen X H, et al. Negative illumination thermoradiative solar cell. Opt Lett, 2017, 42: 3236–3238